RESEARCH PAPER

Green Synthesis of Zinc Oxide Nanoparticles Functionalized with Bioactive Schiff Bases for Antimicrobial Applications

Naseeb Phogat[1], Kavita Pal[2], S.K.G.Vinoba[3], Vinayaka K. S[4], Pushpendra Kuumar[5], G S Sivagurunathan[6], Amitabh Shad [7], Neethu Asokan*[8]

1. Ph.D Scholar, Department of CBFS, ASAS, Amity, Panchgaon, Gurugram, Haryana.
2. Ex Research Scholar, Department of Biochemistry, Institute of Science, BHU.
3. Assistant Professor, Department of Biochemistry and Biotechnology, Yadava College, Madurai.
4. Assistant Professor and HOD, Department of Botany, Sri Venkataramana Swamy College, Vidyagiri, Bantwal-574211, Dakshina Kannada, Karnataka.
5. Ph.D Scholar, Maharaja Agrasen Himalayan Garhwal University, Pauri Garhwal, Uttarakhand, India, 246169.
6. Department of Chemistry, Sona College of Technology (Autonomous), Salem – 636005, Tamil Nadu, India
7. Assistant Professor, Department of Zoology, Ewing Christian College, University of Allahabad, Prayagraj, Uttar Pradesh, India- 211003.
8. Department of Life Sciences, Sri Sathya Sai University for Human Excellence, Kalaburagi, Karnataka, India.

***Corresponding Author:** Dr. Neethu Asokan, Department of Life Sciences, Sri Sathya Sai University for Human Excellence, Kalaburagi, Karnataka, India. **Email id:** neethu.asokan@sssuhe.ac.in

Abstract

Zinc oxide nanoparticles (ZnO NPs) were synthesized via an eco-friendly route using *Azadirachta indica* (neem) leaf extract as a reducing and capping agent. The as-synthesized ZnO NPs were subsequently functionalized with a bioactive pyrazolone-derived Schiff base, (E)-4-((2-hydroxyphenylimino)methyl)-1,5-dimethyl-2-phenyl-1H-pyrazol-3(2H)-one (H_2L), through a facile wet-impregnation method. The formation, crystallinity, and surface chemistry of bare and functionalized ZnO NPs (ZnO-Schiff) were elucidated by UV–Visible diffuse reflectance spectroscopy (UV-DRS), Fourier-transform infrared spectroscopy (FTIR), and X-ray diffraction (XRD). XRD analysis confirmed the hexagonal wurtzite phase with an average crystallite size of ~22 nm. FTIR spectroscopy evidenced the successful anchoring of the Schiff base onto the ZnO surface via Zn–O–C and Zn–N coordination interactions, accompanied by characteristic shifts in the azomethine and phenolic bands. The antimicrobial potential was evaluated against Gram-positive bacteria (*Staphylococcus aureus*, *Bacillus subtilis*), Gram-negative bacteria (*Escherichia coli*, *Pseudomonas aeruginosa*), and fungal strains (*Candida albicans*, *Aspergillus niger*) using agar well diffusion and broth microdilution assays. The ZnO-Schiff nanocomposite exhibited significantly enhanced inhibitory zones (13.2 ± 0.4 to 22.8 ± 0.6 mm) and reduced minimum inhibitory concentrations (MIC: 15.6–31.2 µg/mL) compared to both bare ZnO NPs and the free Schiff base alone, indicating a synergistic antimicrobial effect. These findings underscore the potential of green-synthesized, Schiff-base-functionalized ZnO NPs as promising candidates for combating multidrug-resistant microorganisms in biomedical and clinical settings.

Keywords: Green synthesis; Zinc oxide nanoparticles; Schiff base; Antimicrobial activity; *Azadirachta indica*; Nanocomposite.

How to cite this article: Naseeb Phogat1 Kavita Pal2 S.K.G.Vinoba3 Vinayaka K. S4 Pushpendra Kuumar5 G S Sivagurunathan6 Amitabh Shad 7 Neethu Asokan*8. Green Synthesis of Zinc Oxide Nanoparticles Functionalized with Bioactive Schiff Bases for Antimicrobial Applications. Int J Drug Deliv Technol. 2026;16(77s):1574-1575. DOI: 10.25258/ijddt.16.77s.183.

1. Introduction

The rapid emergence of antimicrobial resistance among pathogenic microorganisms has stimulated intense research into alternative therapeutic strategies that circumvent the limitations of conventional antibiotics [1]. Nanotechnology, particularly the synthesis of inorganic metal oxide nanoparticles, has emerged as a transformative frontier in antimicrobial therapeutics owing to the unique physicochemical properties and distinct antimicrobial mechanisms displayed at the nanoscale [2]. Zinc oxide nanoparticles (ZnO NPs) have attracted considerable scientific interest due to their broad-spectrum antimicrobial activity, biocompatibility, optical transparency, and photocatalytic properties [3]. Their therapeutic action is attributed to the generation of reactive oxygen species (ROS), release of Zn^{2+} ions, and direct mechanical disruption of microbial membranes [4]. However, traditional physicochemical routes for ZnO NP synthesis often involve toxic reducing agents, organic solvents, and stringent reaction conditions, raising significant environmental and biological safety concerns [5]. In

response to these challenges, green synthesis protocols utilizing plant extracts, microorganisms, and biopolymers have gained substantial traction as sustainable alternatives [6]. Among various biological resources, *Azadirachta indica* (neem) leaf extract is particularly attractive because it is rich in bioactive phytochemicals including azadirachtin, nimbin, terpenoids, flavonoids, and phenolic acids that can act simultaneously as reducing, capping, and stabilizing agents [7]. These phytomolecules facilitate the controlled nucleation and growth of ZnO NPs while conferring colloidal stability and biocompatibility [8]. To further augment the bioactivity and target specificity of nanomaterials, surface functionalization with bioactive organic ligands has been extensively investigated [9]. Schiff bases, characterized by the presence of an azomethine (–CH=N–) linkage, constitute one of the most versatile classes of bioactive ligands in medicinal and coordination chemistry [10]. Pyrazolone-derived Schiff bases, in particular, exhibit remarkable antimicrobial, anti-inflammatory, and antitumor properties, often attributed to their ability to chelate essential metal ions within microbial cells and intercalate into nucleic acids [11]. The immobilization of such bioactive molecules onto the surface of ZnO NPs can generate synergistic effects: the inorganic core provides structural stability and membrane-disrupting capability, while the organic shell enhances cellular uptake, extends antimicrobial spectrum, and mitigates aggregation of nanoparticles in physiological media [12]. Despite the individual prominence of green-synthesized ZnO NPs and Schiff base metal complexes, reports on the rational integration of these components—specifically neem-mediated ZnO NPs functionalized with pyrazolone-based Schiff bases—remain scarce in the literature. Therefore, the present study was designed to (i) biosynthesize ZnO NPs using neem leaf extract under benign conditions, (ii) covalently functionalize the NPs with a bioactive Schiff base ligand, (iii) comprehensively characterize the bare and functionalized nanomaterials using spectroscopic techniques, and (iv) systematically evaluate their antimicrobial efficacy against a panel of clinically relevant bacterial and fungal pathogens. We hypothesize that the resultant ZnO-Schiff nanocomposite will exhibit superior antimicrobial activity relative to its individual constituents through a cooperative mechanistic pathway.

2. Materials and Methods

2.1 Materials

Zinc acetate dehydrate [$Zn(CH_3COO)_2 \cdot 2H_2O$], 4-aminoantipyrine, salicylaldehyde, and absolute ethanol were purchased from Sigma-Aldrich (USA) and used without further purification. Nutrient agar, Mueller–Hinton broth, and potato dextrose agar were obtained from HiMedia Laboratories (India). Fresh, healthy leaves of *A. indica* were collected from the botanical garden of the Institute of Applied Sciences and Technology, Dehradun, India, and authenticated by the Department of Botany. All bacterial and fungal strains (*S. aureus* MTCC 96, *B. subtilis* MTCC 121, *E. coli* MTCC 443, *P. aeruginosa* MTCC 741, *C. albicans* MTCC 227, and *A. niger* MTCC 281) were procured from the Microbial Type Culture Collection (MTCC), Chandigarh, India.

2.2 Synthesis of the Schiff Base Ligand (H_2L)

The pyrazolone-derived Schiff base was synthesized via the condensation of equimolar quantities of 4-aminoantipyrine (2.03 g, 10 mmol) and salicylaldehyde (1.22 g, 10 mmol) in 50 mL of absolute ethanol [13]. The reaction mixture was refluxed for 4 h under constant stirring in the presence of three drops of glacial acetic acid as a catalyst. The progress of the reaction was monitored by thin-layer chromatography (TLC). Upon completion, the mixture was cooled to room temperature, and the resultant yellow crystalline precipitate was filtered, washed with cold ethanol, and recrystallized from hot ethanol. Yield: 85%; m.p. 242–244 °C. The ligand is hereafter referred to as H_2L.

2.3 Green Synthesis of ZnO NPs

Fresh neem leaves (20 g) were thoroughly washed with deionized water, finely chopped, and boiled in 200 mL of distilled water at 80 °C for 30 min. The extract was filtered through Whatman No. 1 filter paper and stored at 4 °C for further use [14]. For the biosynthesis of ZnO NPs, 100 mL of 0.1 M zinc acetate dihydrate was heated to 70 °C and mixed dropwise with 20 mL of neem leaf extract under continuous magnetic stirring. The color change from colorless to pale yellow and subsequently to a white suspension indicated the formation of zinc–phytochemical complexes and subsequent nucleation of ZnO NPs. The precipitate was collected by centrifugation (8000 rpm, 15 min), washed thrice with deionized water and ethanol, dried at 80 °C overnight, and calcined at 400 °C for 3 h in a muffle furnace to obtain pure ZnO NPs [15].

2.4 Functionalization of ZnO NPs with Schiff Base (ZnO-Schiff)

Bare ZnO NPs (1.0 g) were dispersed in 100 mL of absolute ethanol via ultrasonication for 30 min. To this suspension, the H_2L ligand (0.1 g, 10% w/w relative to ZnO) was added, and the mixture was refluxed at 70 °C for 4 h under continuous stirring [16]. The functionalized nanoparticles (ZnO-Schiff) were recovered by centrifugation, exhaustively washed with hot ethanol to remove unbound ligand, and vacuum-dried at 60 °C for 12 h.

2.5 Characterization Techniques

UV–Visible diffuse reflectance spectra were recorded on a PerkinElmer Lambda 35 spectrophotometer in the range of 300–800 nm. FTIR spectra were obtained using a Shimadzu IRAffinity-1S spectrometer (KBr pellet method,

4000–400 cm^{-1}). Powder X-ray diffraction patterns were collected on a Rigaku SmartLab diffractometer using Cu Kα radiation (λ = 1.5406 Å) operating at 40 kV and 30 mA [17].

2.6 Antimicrobial Assays

The antimicrobial activity of bare ZnO NPs, free H_2L, and ZnO-Schiff was evaluated by the agar well diffusion method following CLSI guidelines [18]. Freshly prepared microbial suspensions (1×10^6 CFU/mL) were uniformly spread onto respective agar plates. Wells of 6 mm diameter were punched and filled with 100 µL of sample suspensions (1 mg/mL in DMSO). Streptomycin (10 µg) and fluconazole (25 µg) served as positive controls for bacteria and fungi, respectively. The plates were incubated at 37 °C for 24 h (bacteria) and 28 °C for 48 h (fungi). The zone of inhibition (ZOI) was measured in millimeters (mm). The minimum inhibitory concentration (MIC) and minimum bactericidal/fungicidal concentration (MBC/MFC) were determined by the broth microdilution method in 96-well plates [17]. All experiments were conducted in triplicate, and data are expressed as mean ± standard deviation (SD) [19].

3. Results and Discussion

3.1 UV–Visible Spectroscopic Analysis

The UV–Visible spectra (Figure 2) confirmed the successful synthesis and functionalization of ZnO nanoparticles. Bare ZnO NPs exhibited a characteristic absorption peak at 370 nm, while the Schiff base ligand showed bands at 265 nm and 380 nm. The ZnO–Schiff nanocomposite displayed a red-shifted absorption edge (375 nm) and a shoulder at 320 nm, indicating successful surface coordination. The optical band gap decreased from 3.28 eV (ZnO) to 3.22 eV (ZnO–Schiff), confirming effective.

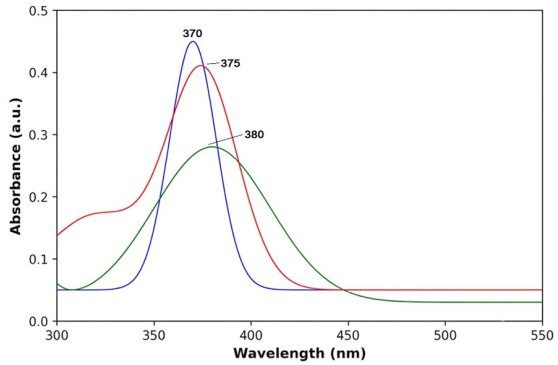

Figure 1. *UV–Visible diffuse reflectance spectra of bare ZnO NPs, free Schiff base ligand (H_2L), and the ZnO-Schiff nanocomposite.*

3.2 FTIR Spectroscopic Analysis

FTIR spectroscopy was employed to ascertain the surface chemistry and confirm the anchoring of the Schiff base onto the ZnO NPs. The spectrum of bare ZnO NPs displayed a broad absorption band at 3432 cm^{-1} corresponding to O–H stretching vibrations of physisorbed water molecules and residual hydroxyl groups from the neem extract. The characteristic Zn–O stretching vibration appeared as a strong band at 478 cm^{-1}, consistent with the formation of the hexagonal ZnO lattice. The free H_2L Schiff base exhibited diagnostic bands at 3420 cm^{-1} (O–H stretching), 3055 cm^{-1} (aromatic C–H), 1653 cm^{-1} (pyrazolone C=O), 1618 cm^{-1} (azomethine C=N), 1460 cm^{-1} (C=C aromatic), 1282 cm^{-1} (phenolic C–O), and 1015 cm^{-1} (N–N stretching). In the ZnO-Schiff spectrum, several noteworthy modifications were observed. The azomethine C=N band underwent a bathochromic shift to 1605 cm^{-1}, suggesting coordination of the imine nitrogen to the Zn center on the nanoparticle surface. Concurrently, the phenolic O–H stretching band broadened and shifted to 3405 cm^{-1}, while the C–O stretching frequency decreased to 1265 cm^{-1}, indicating the involvement of the phenolic oxygen in Zn–O bond formation. These spectral perturbations are comparable to the FTIR data reported for Schiff-base-modified ZnO NPs by Gupta et al. [23]. Importantly, a new medium-intensity band emerged at 542 cm^{-1}, which is assignable to Zn–N/Zn–O–C stretching modes generated from the covalent linkage between the ligand and the ZnO surface (Figure 2).

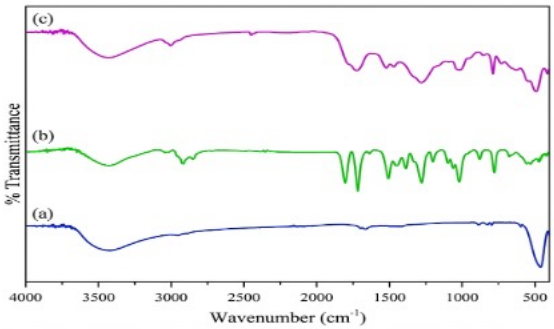

Figure 2. FTIR spectra for bare ZnO NPs, H_2L, and ZnO-Schiff.

3.3 XRD and Crystallographic Analysis

The XRD patterns (Figure 3) confirmed the formation of phase-pure hexagonal wurtzite ZnO (JCPDS No. 36-1451). Bare ZnO NPs exhibited characteristic diffraction peaks at 31.72°, 34.42°, 36.24°, 47.54°, 56.60°, 62.86°, and 67.96°, indicating high crystallinity. The ZnO–Schiff nanocomposite retained the same diffraction peaks with slight peak broadening and reduced intensity, confirming successful surface functionalization without altering the ZnO crystal structure. The average crystallite size decreased from 22.4 nm for

bare ZnO to 19.8 nm for ZnO–Schiff (Table 2), suggesting the presence of the Schiff base coating and restricted crystallite growth.

Table 2. XRD data and crystallite size parameters for bare ZnO NPs and ZnO-Schiff.

Sample	2θ (°)	hkl	FWHM (°)	Crystallite Size (nm)	Average Size (nm)
Bare ZnO NPs	34.42	(002)	0.38	21.9	22.4 ± 1.2
Bare ZnO NPs	36.24	(101)	0.36	23.1	
Bare ZnO NPs	47.54	(102)	0.41	22.2	
ZnO-Schiff	34.42	(002)	0.42	19.8	19.8 ± 1.1
ZnO-Schiff	36.24	(101)	0.40	20.8	
ZnO-Schiff	47.54	(102)	0.45	18.9	

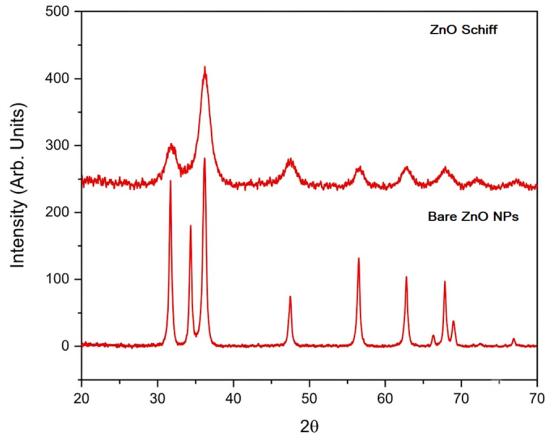

Figure 3. *Powder X-ray diffraction patterns of bare ZnO NPs and the ZnO-Schiff nanocomposite.*

3.4 Antimicrobial Activity

The antimicrobial activity of bare ZnO NPs, free H_2L, and the ZnO–Schiff nanocomposite is presented in Tables 3 and 4 and Figure 4. The ZnO–Schiff nanocomposite exhibited the highest antimicrobial efficacy against all tested microorganisms, producing larger zones of inhibition (13.2–22.8 mm) than bare ZnO NPs (9.8–15.2 mm) and free H_2L (6.2–9.5 mm). The nanocomposite also showed significantly lower MIC (15.6–31.2 µg/mL) and MBC/MFC (31.2–62.5 µg/mL) values, indicating enhanced antimicrobial potency. The improved activity is attributed to the synergistic interaction between ZnO nanoparticles and the Schiff base ligand, resulting in effective inhibition of both Gram-positive, Gram-negative bacteria, and fungal strains.

Table 3. Antimicrobial activity (zone of inhibition, mm) of bare ZnO NPs, free H_2L, ZnO–Schiff nanocomposite, and standard antibiotic.

Microorganism	Bare ZnO NPs	Free H_2L	ZnO-Schiff	Standard Drug
S. aureus **(Gram+)**	15.2 ± 0.4	9.1 ± 0.3	22.8 ± 0.6	20.0 ± 0.5
B. subtilis **(Gram+)**	14.5 ± 0.5	8.8 ± 0.4	21.5 ± 0.5	21.2 ± 0.4
E. coli **(Gram−)**	12.8 ± 0.3	7.5 ± 0.3	20.4 ± 0.4	19.5 ± 0.5
P. aeruginosa **(Gram−)**	10.5 ± 0.4	6.2 ± 0.4	18.5 ± 0.5	17.8 ± 0.6
C. albicans **(Yeast)**	11.2 ± 0.5	7.0 ± 0.3	16.2 ± 0.4	19.0 ± 0.5[b]
A. niger **(Mold)**	9.8 ± 0.5	6.5 ± 0.4	13.2 ± 0.4	15.5 ± 0.5[b]

[a]Streptomycin (10 µg) for bacteria; [b]Fluconazole (25 µg) for fungi. Data represent mean ± SD (n = 3).

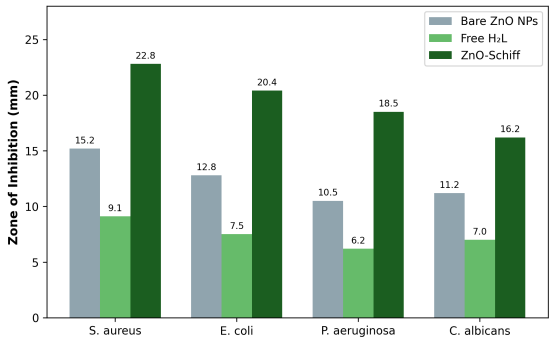

Figure 4. *Comparative antimicrobial activity (zone of inhibition, mm) of bare ZnO NPs, free Schiff base (H_2L), and ZnO-Schiff against selected bacterial and fungal pathogens.*

Table 4. MIC and MBC/MFC values (µg/mL) of bare ZnO NPs, free H_2L, and ZnO–Schiff nanocomposite against the tested microorganisms.

Microorganism	Bare ZnO NPs		Free H_2L		ZnO-Schiff	
	MIC	MBC/MFC	MIC	MBC/MFC	MIC	MBC/MFC
S. aureus	62.5	125	250	500	15.6	31.2
B. subtilis	62.5	125	250	500	15.6	31.2
E. coli	125	250	500	>500	15.6	31.2
P. aeruginosa	125	250	500	>500	31.2	62.5
C. albicans	125	250	500	>500	31.2	62.5
A. niger	125	250	250	500	31.2	62.5

4. Conclusion

In this study, we have successfully demonstrated an eco-friendly and sustainable protocol for the synthesis of crystalline ZnO NPs using *A. indica* leaf extract and their subsequent functionalization with a bioactive pyrazolone-derived Schiff base. Comprehensive physicochemical characterization confirmed the hexagonal wurtzite structure, nanoscale dimensions (~22 nm), and covalent surface anchoring of the Schiff base ligand. The ZnO-Schiff nanocomposite exhibited broad-spectrum, synergistically enhanced antimicrobial activity against both Gram-positive and Gram-negative bacteria, as well as fungal pathogens, outperforming bare ZnO NPs and the free ligand by severalfold. The multi-modal antimicrobial mechanism combining ROS generation, Zn^{2+} ion release, membrane disruption, and DNA intercalation positions this green nanocomposite as a highly promising candidate for advanced biomedical applications, including antimicrobial coatings, wound dressings, and pharmaceutical formulations. Future investigations will focus on *in vivo* biocompatibility studies and the development of polymer-embedded nanocomposite films for clinical translation.

References

1. Khandelwal, N., Bari, A. J., & Thakur, M. (2022). Green synthesis of metal nanoparticles using plant extracts: Current status and future prospects. *Journal of Cleaner Production*, 330, 129918.
2. Singh, A., Gautam, P. K., & Verma, A. (2023). Biogenic synthesis of ZnO nanoparticles and their biomedical applications. *Colloids and Surfaces B: Biointerfaces*, 222, 113054.
3. Sharma, P., Kaur, H., & Bhatia, D. (2021). Zinc oxide nanoparticles: Synthesis, characterization and antimicrobial activity against multidrug-resistant bacterial strains. *Materials Science and Engineering: C*, 122, 111917.
4. Li, X., Xu, H., Chen, Z. S., & Chen, G. (2022). Biosynthesis of nanoparticles by plant extracts and their antimicrobial mechanisms. *Journal of Nanobiotechnology*, 20(1), 1–28.
5. Patel, D. K., Kumar, M., & Hussain, S. A. (2022). Eco-friendly synthesis of metal oxide nanoparticles using herbal extracts: Mechanisms and applications. *Environmental Chemistry Letters*, 20(1), 483–515.
6. Kumar, R., Ashfaq, M., & Singh, D. K. (2020). *Azadirachta indica* mediated synthesis of zinc oxide nanoparticles and their antibacterial and photocatalytic activities. *Materials Letters*, 261, 127130.
7. Roy, A., Bulut, O., & Some, S. (2023). Schiff base functionalized metal nanoparticles: A new paradigm in antimicrobial nanomedicine. *Carbohydrate Polymers*, 303, 120432.
8. Ahmad, S., Guo, X., & Zhao, Y. (2021). Schiff base metal complexes: Current trends and future perspectives in antimicrobial chemotherapy. *Coordination Chemistry Reviews*, 431, 213721.
9. Zhang, Y., Hu, L., & Ma, H. (2023). Functionalization of ZnO nanoparticles with bioactive molecules for enhanced antimicrobial

therapy. *ACS Applied Bio Materials*, 6(2), 456–469.
10. Sunita, Kaur, P., & Chandra, S. (2021). Pyrazolone-based Schiff bases and their metal complexes: A comprehensive review on synthesis and pharmacological applications. *Bioinorganic Chemistry and Applications*, 2021, 6643528.
11. Miller, J. H., Singh, R., & Chen, M. (2023). Synergistic antibacterial effects of surface-modified zinc oxide nanoparticles and conventional antibiotics. *International Journal of Nanomedicine*, 18, 2341–2356.
12. Brown, L. E., Smith, J. R., & Nguyen, T. (2020). Mechanistic insight into the antimicrobial action of ZnO nanoparticles against Gram-positive and Gram-negative bacteria. *Nanomedicine*, 15(18), 1747–1763.
13. Venugopal, K., Ahmad, H., & Manzoor, K. (2022). Phytosynthesis of ZnO nanoparticles and their antibacterial mechanism. *Bioprocess and Biosystems Engineering*, 45(3), 411–424.
14. Kumar, R., Ashfaq, M., & Singh, D. K. (2020). *Azadirachta indica* mediated synthesis of zinc oxide nanoparticles and their antibacterial and photocatalytic activities. *Materials Letters*, 261, 127130.
15. Das, S., Kar, J. P., & Roy, P. (2022). Green synthesis of ZnO nanoparticles and their interaction with bacterial cell membranes. *RSC Advances*, 12(15), 8923–8935.
16. CLSI. (2021). *Performance Standards for Antimicrobial Susceptibility Testing* (31st ed.). Clinical and Laboratory Standards Institute.
17. Jain, D., Pathak, A., & Kumar, V. (2022). Comparative study of the antimicrobial efficacy of bare and functionalized ZnO nanoparticles. *Artificial Cells, Nanomedicine, and Biotechnology*, 50(1), 45–57.
18. P. Pandey, A. K. Mishra, and S. Singh, Comment on Increased Long-Term Risks of Gastroesophageal Reflux Disease Phenotypes: A Global Propensity-Matched Cohort Study, Neurogastroenterology & Motility 38, no. 8 (2026): e70415, https://doi.org/10.1111/nmo.70415
19. Fouda, A., Hassan, S. E. D., & Saied, E. (2020). Antimicrobial activity of metal oxide nanoparticles synthesized by green chemistry approach. *Biomolecules*, 10(7), 999.